

# 64-Meter Antenna Operation at $K_A$ -Band

P. D. Potter

Radio Frequency and Microwave Subsystems Section

*As a part of a FY-80 study of the future potential of the 32-GHz  $K_A$ -band frequency region to planetary exploration, this article addresses the expected performance of the 64-m antenna network at 32 GHz. A modest level of noninterference upgrade work is assumed to achieve reasonable antenna aperture efficiency and alleviate antenna pointing difficulties. As a final item, electronic compensation of antenna aperture phasing errors is briefly considered as an alternative to the physical upgrade.*

## I. Introduction

Communications is clearly a vital factor in the planetary exploration program. As a dramatic example of improvements made during the last 20 years, the 1959 Pioneer IV Lunar probe with its 0.27-W transmitter could have transmitted from a distance of one AU at a data rate of only 0.00025 bit/s to the then existing 26-m ground antenna; whereas on March 5, 1979, Voyager I transmitted from a distance of 4.5 AU (Jupiter) at a rate of 115,200 bit/s to a 64-m ground antenna. This spectacular improvement of 100 dB represents an overall average of 5 dB per year. In addition to the larger ground antenna aperture (7.9 dB), a higher frequency (8.5 GHz as opposed to 0.96 GHz) and a larger spacecraft antenna combined to provide a spacecraft antenna gain improvement of 45.6 dB. Other major improvements were made in transmitted power, receiving system effective noise temperature, and information coding efficiency. Major future improvements in these last three areas are unlikely, since rather basic limitations have been approached.

Looking to the future, it appears that the most fruitful areas for link capability improvement lie in the increase of

ground antenna aperture and spacecraft antenna gain. Present plans call for enhancement of ground aperture by the arraying of existing antenna equipments. Further ground improvement by construction of additional aperture area, however, is expensive and does not presently appear probable. Enhancement of the spacecraft antenna gain by use of large unfurlable antennas is technically feasible; however, this approach is associated with severe spacecraft configuration constraints, weight penalty, and mission reliability questions. A more practical approach is to increase spacecraft antenna gain by use of a higher frequency.

In 1969, JPL performed a general study of possible frequency bands for future deep-space-to-Earth data links (Ref. 1). Four frequency bands were studied in detail: 8.5 GHz (3.5-cm wavelength), 90 GHz (3.3-mm wavelength), 10  $\mu\text{m}$  (coherent carbon dioxide laser system), and a 0.87- $\mu\text{m}$  gallium arsenide "photon bucket" laser system. This study was unique in that, by definition, all four systems had exactly equal link performances; with this technique, the relative attractiveness of each system was clearly displayed. A highly-visible output of the JPL study was that, compared with the

microwave region, the infrared and optical (laser) frequency region is not attractive for a deep-space-to-Earth communications link. This conclusion, still valid in 1980, derives from basic considerations of high noise level, poor daytime performance, severe logistics problems (site selection), total weather dependency, severe spacecraft pointing problems, and poor hardware component technology.

The  $K_A$ -band and (32-GHz) frequency region has become increasingly attractive recently by virtue of a number of technical advances: the proven reliability and high efficiency of the 64-m antenna network at 8.5 GHz, demonstration of K-band low noise maser receiver designs (Ref. 2), demonstration of the low surface error Voyager spacecraft antenna, and availability of suitable  $K_A$ -band travelling wave tube spacecraft transmitter devices. Finally, this frequency band is attractive from a microwave components standpoint: the 1-cm wavelength is compatible with normal manufacturing tolerances and quality control considerations. From a system standpoint, the  $K_A$ -band represents a 4:1 step from the existing X-band system, large enough for a substantial link performance enhancement, but not large enough to require new or radically different technology. The associated reduced spacecraft antenna beamwidth, however, does impact the spacecraft design in terms of a more stringent antenna pointing requirement. This problem is being studied as a part of this task.

## II. The Effect of Atmospheric Turbulence at $K_A$ -Band

The ground antenna effective aperture would remain essentially constant with increasing frequency were it not for the effect of aperture phase distortions, the so-called "Ruze" effect (Refs. 3 and 4), which becomes serious (4-dB loss) as the standard deviation of these phase distortions approaches 1/12 wavelength. Mechanical deflections, manufacturing tolerances, and small-scale tropospheric turbulence all result in more or less random phase errors whose associated aperture efficiency loss factor,  $\eta_s$ , is given by (Ref. 4):

$$\eta_s = e^{-\left(\frac{4\pi\sigma}{\lambda}\right)^2} \quad (1)$$

where

$\sigma$  = standard deviation of the one-half path-length error

$\lambda$  = wavelength

It should be noted that, because of the exponential form of Eq. (1), if several statistically independent aperture phase

errors exist, then the total loss in dB is simply the sum of the individual losses in dB.

The effect of tropospheric inhomogeneities in perturbing the incoming wavefront is depicted in Fig. 1. Curiously, it can be seen that the aperture precision quantity,  $\sigma/D$ , decreases with larger aperture sizes, whereas this quantity generally *increases* as a function of antenna size for physical distortions. For the small scale case, Ruina and Angula (Ref. 5) derived a simple expression for the associated standard deviation of the 1/2 pathlength variation,  $\sigma_{ss}$ :

$$\sigma_{ss} = 0.5 (Rz_0)^{1/2} \delta \quad (2)$$

where

$R$  = effective path length through the turbulent region

$z_0$  = inhomogeneity scale size

$\delta$  = rms fractional index of refraction variation of the inhomogeneities

For the large scale case, they derived a simple expression for rms wavefront tilt,  $\beta$ :

$$\beta = \left(\frac{2R}{z_0}\right)^{1/2} \delta, \text{ rad} \quad (3)$$

The antenna power gain function,  $G(\beta)$  may be conveniently expressed in a Gaussian form:

$$G(\beta) \equiv e^{-\alpha\left(\frac{\beta}{B}\right)^2} = e^{-\alpha\left(\frac{D\beta}{\lambda}\right)^2} \quad (4)$$

where

$B$  = antenna beamwidth, rad

$\alpha = \ln(2)/0.25 = 2.77$

$D$  = antenna diameter

$\lambda$  = wavelength

For large-scale inhomogeneities, an equivalent "Ruze Loss" standard deviation  $\sigma_{1s}$  may be defined such that the  $G(\beta)$  loss given by Eq. (4) equals the loss predicted by Eq. (1) for  $\sigma_{1s}$ . When this is done, and the result combined with Eq. (3), the following result is obtained:

$$\sigma_{1s} = \frac{(2\alpha)^{1/2}}{4\pi} \left(\frac{R}{z_0}\right)^{1/2} D\delta = 0.187 \left(\frac{R}{z_0}\right)^{1/2} D\delta \quad (5)$$

If the turbulence scale size,  $\epsilon_0$ , is small compared to the aperture size,  $D$ , then Eq. (2) is the appropriate relationship to use; if  $\epsilon_0$  is large compared to  $D$ , then Eq. (5) is appropriate. Typically (Ref. 6),  $R = 1.8 \times 10^4$  m (10-deg elevation),  $\epsilon_0 = 40$  m, and  $\delta = 0.4 \times 10^{-6}$ . Figure 2 shows the resulting  $\sigma/D$  value as a function of antenna diameter for 10- and 30-deg elevation angles. These calculations are semiquantitatively confirmed by 1969 National Radio Astronomy Observatory (NRAO) tropospheric phase stability tests (Ref. 7), which showed a  $\sigma$  of 0.3 to 0.45 mm for baselines up to 300 m. The troposphere thus behaves in a well understood way in its distortion of a signal wavefront, and, as shown in Table 1, does not seriously degrade a  $K_A$ -band 64-m antenna system.

### III. 64-m Antenna Aperture Efficiency at $K_A$ -Band

Three modifications to the 64-m antennas are assumed to provide  $K_A$ -band usability: (1) a new precision subreflector, (2) new precision surface panels, and (3) reduction of the gravity-induced surface errors over the elevation wheel assembly. A practical technique for reduction of the gravity errors was studied by Katow (Ref. 8). Katow presented zenith look and horizon look gravity off-on distortions of 0.43 mm and 0.46 mm, respectively. The resulting gravity distortions are elevation-angle dependent, and are given to good approximation by:

$$\sigma_G^2 = \sigma_H^2 (\cos \theta - \cos \theta_s)^2 + \sigma_Z^2 (\sin \theta - \sin \theta_s)^2 \quad (6)$$

where

- $\sigma_G$  = rms surface error due to gravity
- $\sigma_H$  = rms gravity off-on horizon distortion
- $\sigma_Z$  = rms gravity off-on zenith distortion
- $\theta$  = antenna elevation angle
- $\theta_s$  = elevation angle at which the panels are set

Table 1 collects the various estimates of surface distortion, the troposphere turbulence effect, and the effect of a 0.001-deg rms pointing error (Ref. 9). By combining Eqs. (1) and (4), the  $\sigma$  equivalent in mm of a 64-m antenna pointing error is found to be 150 times the rms pointing error in degrees. Figure 3 shows the aperture efficiency as a function of frequency for the  $\sigma$ 's in Table 1, as predicted by Eq. (1).

### IV. Electronic Surface Error Compensation

In principle, aperture phasing errors may be compensated electronically by use of an extended adaptive feed. Such an

approach provides an alternative to the structural upgrade described in the previous section. A multielement feed is not necessarily incompatible with low receiving system effective noise temperature. Refrigeration techniques (Ref. 10) may be used to reduce dissipative losses and their effect.

In 1970, Rudge and Davies (Ref. 11) published a detailed analysis of electronic surface error compensation and reported promising experimental results. The novel feature of the Rudge-Davies feed is that a Fourier transform of the focal plane array feed outputs is performed, thereby reconstructing the aperture distribution. Since the receive aperture distribution is constant in amplitude (but not in phase), it can be readily corrected to the ideal uniform phase distribution by a set of phase shifters and then inverse Fourier transformed to thus reconstruct the output that would result with no surface errors. The Rudge-Davies implementation was nonadaptive and used Butler Matrices (Ref. 12) to perform analog Fourier transforms.

An alternative adaptive mechanization would involve a microwave Butler Matrix to provide the first Fourier transformation and a multichannel phase-sensitive receiver to correct phase errors (see Ref. 13 for receiver details). Because of its versatility and apparent compatibility with existing 64-m antenna surface errors, an electronically compensated feed system is attractive; its technical feasibility remains to be demonstrated, however.

### V. Electronic Beam Pointing

The electronic system described in the previous section can compensate for pointing errors. If such a system is not used, i.e., the physical upgrade approach is selected, then an electronic pointing system can be used to achieve reliable pointing accuracies of less than 0.001 deg. This system, described in a previous article (Ref. 14) uses higher-order corrugated waveguide modes to achieve the desired antenna beam squint to compensate for physically induced pointing errors. The required mode amplitudes and phases are established by a system of semiconductor waveguide probes or couplers. Such a system may be implemented either as a conscan or as a monopulse system, or perhaps an operator-selectable system.

### VI. Conclusion

There does not appear to be any serious difficulty in upgrading the DSN 64-m antenna network to operate efficiently at  $K_A$ -band (32 GHz). This may be achieved either by conventional physical upgrade, or by use of advanced electronic techniques.

## References

1. Potter, P. D., Shumate, M. S., Stelzried, C. T., and Wells, W. H., *A Study of Weather-Dependent Data Links for Deep Space Applications*, Technical Report No. 32-1392, Jet Propulsion Laboratory, Pasadena, Calif., October 15, 1969.
2. Moore, C. R., and Clauss, R. C., "A Reflected - Wave Ruby Maser with K-Band Tuning Range and Large Instantaneous Bandwidth," *IEEE Transactions on Microwave Theory and Techniques*, Vol. MTT-27, No. 3, pp. 249-256, March, 1979.
3. Ruze, J., *Physical Limitations on Antennas*, Technical Report No. 248, Research Laboratory of Electronics, MIT, Astia Document 62351, October, 1952.
4. Ruze, J., "Antenna Tolerance Theory—A Review," *Proceedings of the IEEE*, Vol. 54, No. 4, pp. 633-640, April, 1966.
5. Ruina, J. P., and Angulo, C. M., "Antenna Resolution as Limited by Atmospheric Turbulence," *IEEE Transactions on Antennas and Propagation*, Vol. AP-11, No. 2, pp. 153-161, March, 1963.
6. Crain, C. M., Straiton, A. W., and Von Rosenberg, C. E., "A Statistical Survey of Atmospheric Index-of-Refractive Variation," *IRE Transactions on Antennas and Propagation*, Vol. AP-1, No. 2, pp. 43-46, October, 1953.
7. Basart, J. P., Miley, G. K., and Clark, B. G., "Phase Measurements with Interferometer Baselines of up to 35 km," *National Radio Astronomy Observatory, VLA Scientific Memorandum No. 12*, June 4, 1969.
8. Katow, M. S., "A Proposed Method of Reducing the Gravity Distortions of the 64-Meter Antenna Main Reflector," *JPL Deep Space Network Progress Report No. 42-23*, July - August, 1974, pp. 92-97.
9. Ohlson, J. E., and Reid, M. S., *Conical-Scan Tracking with the 64 m-Diameter Antenna at Goldstone*, Jet Propulsion Laboratory Technical Report No. 32-1605, October 1, 1976.
10. *Final Report, Refrigerated Transmission Line Study, Volumes I and II*, Rantec No. 66327-FR, The Rantec Corporation, Calabasas, California.
11. Rudge, A. W., and Davies, D. E. N., "Electronically Controllable Primary Feed For Profile-Error Compensation of Large Parabolic Reflectors," *Proceedings of the IEE (British)*, Vol. 117, No. 2, February, 1970, pp. 351-358.
12. Butler, J., and Lowe, R., "Beam Forming Matrix Simplifies Design of Electronically Scanned Antennas," *Electronic Design*, Vol. 9, pp. 170-173.
13. Brockman, M. H., "Radio-Frequency Carrier Arraying for High-Rate Telemetry Reception," *JPL Deep Space Network Progress Report No. 42-45*, March and April 1978, pp. 209-223.
14. Potter, P. D., "Feasibility of Inertialess Conscan Utilizing Modified DSN Feed Systems," *JPL Deep Space Network Progress Report 42-51*, June, 1979, pp. 85-93.

**Table 1. Upgraded 64-m antenna 1/2 pathlength errors and associated 32-GHz gain losses**

Error mechanism	Elevation angle					
	Zenith		30 deg		10 deg	
	$\sigma$ , mm	Loss, dB	$\sigma$ , mm	Loss, dB	$\sigma$ , mm	Loss, dB
Gravity (structure)	0.42	-1.38	0.038	-0.01	0.19	-0.28
Wind (32 km/hr) <sup>a</sup>	0.28	-0.61	0.28	-0.61	0.28	-0.61
Subreflector <sup>a</sup> manufacturing	0.25	-0.49	0.25	-0.49	0.25	-0.49
Panel <sup>a</sup> manufacturing	0.25	-0.49	0.25	-0.49	0.25	-0.49
Panel <sup>a</sup> setting	0.25	-0.49	0.25	-0.49	0.25	-0.49
Tropospheric turbulence	0.12	-0.11	0.18	-0.25	0.30	-0.70
Antenna pointing	0.15	-0.17	0.15	-0.17	0.15	-0.17
<b>TOTALS</b>	<b>0.69</b> (RSS)	<b>-3.74</b>	<b>0.57</b> (RSS)	<b>-2.51</b>	<b>0.64</b> (RSS)	<b>-3.23</b>

<sup>a</sup>Estimates provided by M. S. Katow of the JPL DSN Engineering Section.

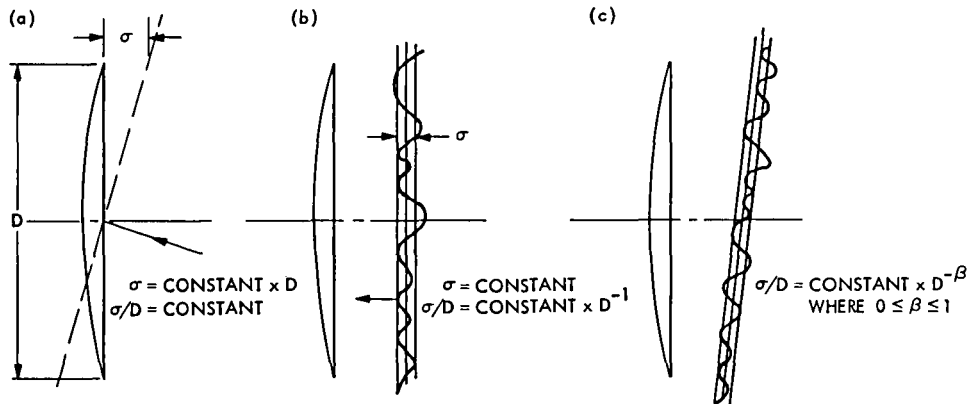


**Fig. 1. Effect of scale size on tropospheric distortion effect: (a) model of large-scale wavefront distortion; (b) model of small-scale wavefront distortion; (c) model of the general case**

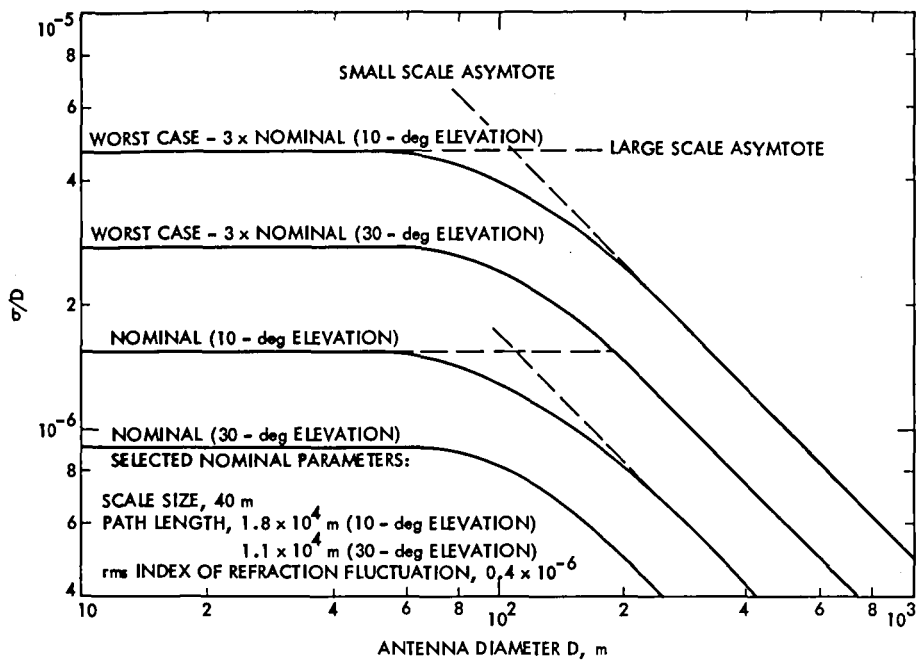


Fig. 2.  $\sigma/D$  equivalent of the troposphere

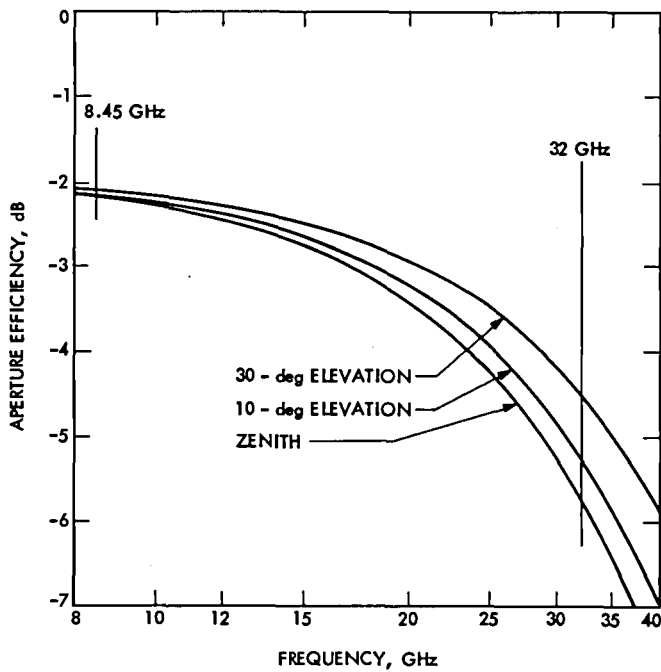


Fig. 3. Upgraded 64-m antenna aperture efficiency vs frequency